KISS1R Intracellular Trafficking and Degradation: Effect of the Arg386Pro Disease-Associated Mutation

Suzy D. C. Bianco, Lauren Vandepas, Mayrin Correa-Medina, Balázs Gereben, Abir Mukherjee, Wendy Kuohung, Rona Carroll, Milena G. Teles, Ana Claudia Latronico, and Ursula B. Kaiser

Department of Molecular and Cellular Pharmacology (S.D.C.B.) and Division of Endocrinology and Metabolism (S.D.C.B., L.V., M.C.-M.), University of Miami Miller School of Medicine, Miami, Florida 33136; Laboratory of Endocrine Neurobiology, Institute of Experimental Medicine (B.G.), Hungarian Academy of Sciences, Budapest, Hungary; Developmental Endocrinology Unit, Laboratory of Hormones and Molecular Genetics (M.G.T., A.C.L.), Teaching Hospital of the University of São Paulo Medical School, São Paulo, Brazil; and Division of Endocrinology, Diabetes, and Hypertension (A.M., W.K., R.C., U.B.K.), Brigham & Women's Hospital and Harvard Medical School, Boston, Massachusetts 02115

The goal of this study was to investigate how the Arg386Pro mutation prolongs KiSS-1 receptor (KISS1R) responsiveness to kisspeptin, contributing to human central precocious puberty. Confocal imaging showed colocalization of wild-type (WT) KISS1R with a membrane marker, which persisted for up to 5 h of stimulation. Conversely, no colocalization with a lysosome marker was detected. Also, overnight treatment with a lysosome inhibitor did not affect WT KISS1R protein, whereas overnight treatment with a proteasome inhibitor increased protein levels by 24-fold. WT and Arg386Pro KISS1R showed time-dependent internalization upon stimulation. However, both receptors were recycled back to the membrane. The Arg386Pro mutation did not affect the relative distribution of KISS1R in membrane and internalized fractions when compared to WT KISS1R for up to 120 min of stimulation, demonstrating that this mutation does not affect KISS1R trafficking rate. Nonetheless, total Arg386Pro KISS1R was substantially increased compared with WT after 120 min of kisspeptin stimulation. This net increase was eliminated by blockade of detection of recycled receptors, demonstrating that recycled receptors account for the increased responsiveness of this mutant to kisspeptin. We therefore conclude the following: 1) WT KISS1R is degraded by proteasomes rather than lysosomes; 2) WT and Arg386Pro KISS1R are internalized upon stimulation, but most of the internalized receptors are recycled back to the membrane rather than degraded; 3) the Arg386Pro mutation does not affect the rate of KISS1R trafficking—instead, it prolongs responsiveness to kisspeptin by decreasing KISS1R degradation, resulting in the net increase on mutant receptor recycled back to the plasma membrane. (*Endocrinology* 152: 1616–1626, 2011)

A hallmark of puberty initiation is an increase in pulsatile secretion of hypothalamic GnRH. The recent identification of KiSS-1 receptor (KISS1R), a G protein–coupled receptor (GPCR), and its natural ligand, kisspeptin, as powerful regulators of GnRH secretion has led to the hypothesis that this ligand/receptor system serves as a gatekeeper of puberty (1–7). Inactivating mutations of KISS1R are associated with hypogonadotropic hypogonadism (8–11), and a gain-of-function mutation of this

receptor (Arg386Pro) was recently associated with human central precocious puberty (12). This gain-of-function mutation accelerates puberty by prolonging responsiveness to kisspeptin through regulation of KISS1R signaling activity (12).

Similar to most GPCRs, KISS1R signaling is terminated by ligand-induced desensitization, which is an essential feedback step in the regulation of receptor activity (13–17). Acute desensitization of GPCRs is due to uncoupling

Abbreviations: CFP, Cyano-fluorescent protein; CHO, Chinese Hamster Ovary; FITC, fluorescein; GPCR, G protein–coupled receptor; KISS1R, KiSS-1 receptor; WT, wild type.

from the signaling pathway, which is usually followed by receptor internalization (18). Internalized receptors are sorted for recycling or destruction, the latter being responsible for long-term GPCR desensitization (18). Desensitization pathways control the extent of the biological effect and are thus strongly regulated (19). An initial robust increase in serum LH in response to kisspeptin administration was shown to desensitize after 3 h, despite continuous presence of ligand. This desensitization was specific for kisspeptin, because LH secretion stimulated by other secretagogues was preserved (16). Similarly, the response of gonadotropins to continuous kisspeptin treatment is desensitized in female rats, an effect shown to be upstream of the pituitary gland, at the hypothalamic GnRH neuron (13). Additionally, Thompson *et al.* showed that gonadotropes are desensitized by continuous kisspeptin treatment in male rats, resulting in testicular degeneration (14).

These observations underscore the importance of KISS1R desensitization for the role of this receptor in timing the onset of puberty and maintaining reproductive capability. Also, disturbances of normal KISS1R desensitization are shown to result in clinical disorders, such as the gonadotropin-dependent precocious puberty found in a female patient carrying the Arg386Pro mutation in KISS1R. In this case, responsiveness to kisspeptin is prolonged as a consequence of delayed desensitization of KISS1R signaling by the Arg386Pro mutation (12). KISS1R was recently shown to internalize rapidly upon kisspeptin stimulation in cells endogenously expressing the receptor (20), suggesting that receptor internalization is involved in short-term KISS1R desensitization. We herein determine the rate of KISS1R internalization and test whether this rate is affected by the Arg386Pro mutation. We also describe the involvement of the proteasome system on long-term desensitization/degradation of the wild-type KISS1R.

Materials and Methods

Reagents

GenePORTER Transfection Reagent was from Gene Therapy Systems (San Diego, CA) and the anion-exchange columns from Bio-Rad (cat # AG1-8X). Antibodies against Na^+K^+ATPase, Lamp2, and fluorescent antibodies were from Abcam (Cambridge, MA); anti-myc and agarose-conjugated anti-myc antibodies from Millipore (Temecula, CA); radioisotopes from Perkin-Elmer (Waltham, MA); and cell culture medium from Mediatech, Inc. (Manassas, VA). Kisspeptin peptides were synthesized by Tufts Medical Center Core Facility (Boston, MA), and all other chemicals were from Sigma-Aldrich (St. Louis, MO).

Expression vectors

Transient expression of KISS1R was performed using the full-length human KISS1R cDNA cloned into the pCMV SPORT6 expression vector as previously described (19). MYC- and cyano-fluorescent protein (CFP)-tagged KISS1Rs were used for transient expression. The 13–amino acid MYC-tag was fused to the amino terminus of KISS1R. MYC-KISS1R was cloned into the PC2$^+$ expression vector. The sequence of the hybrid construct was confirmed. CFP-KISS1R was generated by fusing the amino terminus of CFP to the carboxyl terminus of the human KISS1R. The coding sequence of KISS1R was inserted between the EcoR1 and BamH1 restriction sites of pECFP-N1 vector (Clontech, Mountain View, CA). The sequence of the CFP-KISS1R construct was confirmed. The ubiquitin expression vector used was provided by Dr. Antonio C. Bianco (21).

Inositol phosphate assay

Total inositol phosphates were measured as previously described (12) with slight modifications. The time-course was determined in Chinese Hamster Ovary (CHO) cells stably expressing KISS1R (CHO-KISS1R) (22), whereas dose-response to kisspeptin was measured in COS-7 cells transiently expressing 50 ng of wild-type (WT), MYC-KISS1R, or CFP-KISS1R plus 950 ng control vector, optimized for transfection efficiency. Twenty-four hours after transfection of COS-7 cells or seeding of CHO-KISS1R, cells were inositol-starved for 2 h before the addition of myo-[2-^{3}H]-inositol in inositol-free medium. After overnight incubation, CHO-KISS1R cells were stimulated with 10^{-9} M kisspeptin for 0–18 h at 37 C (time-course), whereas COS-7 cells were stimulated with 10^{-10} to 10^{-7} M kisspeptin for 2 h at 37 C (dose-response). Stimulation was stopped by lysis with 20 mM formic acid. Cells were harvested, neutralized with 7.5 mM HEPES/150 mM KOH, and centrifuged at 14,000 rpm for 5 min at 4 C. Supernatant was applied into anion-exchange columns, washed with water then with 5 mM Borax/60 mM sodium formate before elution of inositol phosphates with 0.9 M ammonium formate/0.1 M formic acid. ^{3}H-inositol was counted and normalized to protein content.

KISS1R membrane trafficking

Internalization and recycling of KISS1R was measured in CHO-KISS1R cells or in COS-7 cells transiently expressing 0.5 μg of WT or Arg386Pro KISS1R + 0.5 μg of control vector. 100,000 cpm of ^{125}I-kisspeptin was added to CHO-KISS1R cells 24 h after seeding or to COS-7 cells 48 h after transfection. After 2–4 h equilibration with radioligand on ice, cells were incubated at 37 C for 0–120 min. Detection of freshly recycled receptors was blocked by replacing unbound radioligand with media before incubation at 37 C or by 30-min treatment with monensin before addition of radioligand. Incubation at 37 C was stopped by moving cells to ice and washing five times with PBS containing 0.5% BSA. Membrane-bound ^{125}I-kisspeptin was extracted by a 3-min incubation with 50 mM acetic acid. Internalized ^{125}I-kisspeptin was collected after lysis with 0.2 M NaOH. Protein was determined by the Bradford method in 10 μl of lysate. Specific ^{125}I-kisspeptin binding was normalized to protein content. Rate of KISS1R trafficking is represented as relative percentile distribution of receptors in the membrane or internalized on each time point, where the total is the combined amount of membrane plus internalized at that time point; net KISS1R is expressed as cpm/mg protein or as ratio of total Arg386Pro:WT.

Displacement of ^{125}I-kisspeptin in cells expressing tagged KISS1R

Binding properties of tagged receptors were tested in COS-7 cells expressing 0.5 μg of MYC-, CFP-, or untagged KISS1R plus 0.5 μg control vector. Cells were incubated for 20 min with 100,000 cpm ^{125}I-kisspeptin plus unlabeled kisspeptin at concentrations ranging from 10^{-10} to 10^{-6} M (2×10^{-5} M for nonspecific binding). Medium was aspirated on ice; cells were washed five times with PBS and lysed with 0.2 M NaOH. Specific binding was normalized to protein content and is represented as percentage of maximal binding (binding at time zero).

Immunofluorescence detection of tagged KISS1R

COS-7 cells in four-well slides were transfected with MYC- or CFP-tagged KISS1R (300 ng KISS1R plus 300 ng control vector). Internal controls were transfected with control vector or untagged KISS1R alone. Forty-eight hours after transfection, cells were stimulated with 10^{-7} M kisspeptin for 0, 5, 10, 15, 30, 60, 120, 180, 240, or 300 min. Stimulation was stopped on ice and slides were washed, fixed with 3.7% p-formaldehyde for 20 min at room temperature, and permeabilized with 0.2% Triton X-100 for 10 min. Washed slides were incubated for 1 h with blocking solution (PBS + 5% BSA), followed by overnight incubation with Alexa488-conjugated anti-myc (1:1,000) or anti-CFP (fixation and permeabilization bleach fluorescence emission by CFP; thus, a fluorescein (FITC)-conjugated anti-GFP antibody that recognizes CFP was used to visualize CFP-KISS1R. This antibody will be referred to throughout as anti-CFP antibody) conjugated to FITC (1:500) at 4 C. Slides were washed and incubated with rabbit polyclonal antibodies against markers of plasma membrane (Na^{+}K^{+}ATPase, 1:500) or late endosome/lysosome (Lamp2, 1:500) for 1 h at room temperature followed by another hour of incubation with Alexa-568–conjugated antirabbit antibody (red) (1:500). Slides were washed, mounted in medium containing 4′,6-diamidino-2-phenylindole (DAPI), and analyzed by confocal microscopy.

Immunoprecipitation and Western-blot analysis of KISS1R

COS-7 or HEK-293 cells were transfected with 0.5 μg MYC-KISS1R + 0.5 μg control vector or 1 μg control vector alone. Forty-eight hours later, some cells were treated with 100 μg/ml leupeptin (lysosome inhibitor) for 16 h or 10 μM MG132 (proteasome inhibitor) for 2 h or 16 h at 37 C. Cells were lysed on ice with 20 mM HEPES containing 1% Nonindet P-40, 1 mM EDTA (EDTA), 150 mM sodium chloride (NaCl), 0.25% sodium deoxycholate, and protease inhibitors. Cell lysates were passed through a 20-gauge needle, incubated for 1 h, and centrifuged at 12,000 *g* for 10 min at 4 C. Supernatants were diluted to 1 mg/ml with PBS and incubated overnight with agarose-conjugated monoclonal anti-myc antibody (4 μg) at 4 C. Immunocomplexes were precipitated, washed three times with lysis buffer, resuspended in sample buffer, and separated on a 4–15% gradient gel. Proteins were transferred to polyvinylidene fluoride (PVDF-FL) membrane (Bio-Rad), and nonspecific binding was blocked with Odyssey Blocking Buffer (LI-COR Biosciences, Lincoln, NE) for 1 h at room temperature before the addition of a rabbit anti-myc antibody (Millipore, 1:500 in Odyssey Blocking Buffer containing 0.1% Tween-20). After overnight incubation at 4 C, membrane was washed and incubated with an antirabbit fluorescent labeled IRDye-800CW (1:5,000) in Odyssey Blocking Buffer

containing 0.1% Tween-20 and 0.01% SDS for 1 h at room temperature. Unincorporated secondary antibody was removed and membranes were scanned and analyzed using the Licor Odyssey Infrared Imaging System (LI-COR Biosciences).

Statistical analysis

Statistical significance was validated when $P < 0.05$. P values were determined by Student's *t* test (two groups comparisons) or ANOVA followed by the Dunnett's comparison for multiple samples.

Results

KISS1R is desensitized and internalized in a time-dependent manner

We have shown previously that KISS1R signaling is desensitized upon continuous kisspeptin stimulation. This was confirmed here in CHO-KISS1R cells, using total inositol phosphate production as a marker of KISS1R signaling. Inositol phosphate levels peaked after 2 h of stimulation, declining thereafter and returning to baseline levels by 12 h, despite continuous presence of kisspeptin. This decline corresponds to the time-dependent desensitization of this signal (Fig. 1A).

To investigate mechanisms involved in this desensitization, we measured the rate of WT KISS1R trafficking (internalization/recycling). Membrane receptors in CHO-KISS1R cells were labeled and tracked using radioactive ligand. After internalization, receptors remain labeled until recycling or degradation. The rate of receptor trafficking thus represents the relative distribution of receptors in membrane and intracellular fractions at specified time points.
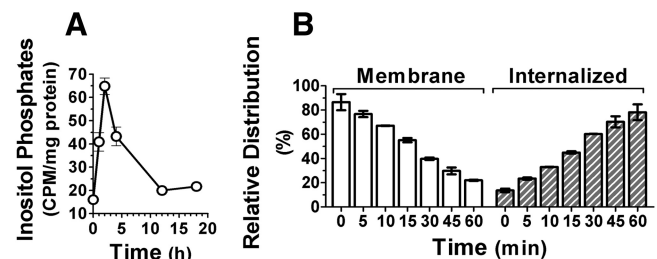

FIG. 1. KISS1R signaling and trafficking in CHO-KISS1R cells. A, Time course of total inositol phosphate production in response to kisspeptin. CHO-KISS1R cells were stimulated with 10^{-9} M kisspeptin for 0–18 h and lysed. Total inositol phosphates were extracted and normalized to protein content. Data are the mean $\pm$ SE of triplicate samples from a representative experiment, repeated at least three times with similar results. B, Rate of KISS1R trafficking. CHO-KISS1R cells were equilibrated on ice with 100,000 cpm of ^{125}I-kisspeptin followed by incubation at 37 C for 0–60 min as indicated. Membrane-bound ^{125}I-kisspeptin was extracted by acidic wash and internalized ^{125}I-kisspeptin was collected after cell lysis. Distribution of ^{125}I-kisspeptin in the membrane (*open bars*) and internalized (*hatched bars*) fractions is represented as relative percentage of ^{125}I-kisspeptin at specific time points as indicated. Results are the mean $\pm$ SEM of three independent experiments.

A time-dependent decrease in membrane binding was observed after incubation of CHO-KISS1R cells with ^{125}I-kisspeptin. This decrease correlated well with proportional increases in internalized receptors (Fig. 1B). Equilibration on ice suppresses cell metabolism thus preventing receptor internalization. Interestingly, about 14% of KISS1R was internalized at time zero (*i.e.*, after equilibration on ice but before incubation at 37 C), indicating that KISS1R is still able to internalize, albeit at a slower rate, at 4 C. Internalization was faster at 37 C and after 15 min at this temperature 50% of the KISS1R was internalized, whereas after 60 min ∼80% of the KISS1R was internalized and only ∼20% remained on the cell surface (Fig. 1B). These results confirm and explain the time-dependent desensitization of KISS1R signaling, as well as confirm involvement of internalization in ligand-mediated desensitization of KISS1R.

KISS1R is localized to the plasma membrane but not to lysosomes

Colocalization of MYC-KISS1R with a plasma membrane marker (Na$^+$K$^+$ATPase) was observed at baseline (Fig. 2, A–C) and persisted for up to 5 h of stimulation with 10^{-7} M kisspeptin, at all time points tested. A representative stimulation point (3 h) is shown in Fig. 2, D–F. This persistent membrane localization was unexpected and suggests a pattern of dynamic recycling of KISS1R back to the membrane after internalization (rather than degradation). Despite the persistent membrane localization, internalization was also visible at all time points. A small degree of internalization was evident at baseline (Fig. 2, A–C), whereas at 3 h stimulation about 25% of receptors were intracellular (Fig. 2, D–F). However, there was no detectable colocalization of CFP-KISS1R (Fig. 2, G–I) or MYC-KISS1R (not shown) with a late endosome/lysosome marker (Lamp2) at any of the time points tested (0–5 h), suggesting a lack of lysosomal targeting and degradation of KISS1R. A representative coimmunostaining of CFP-KISS1R and Lamp2 (at baseline) is shown in Fig. 2, G–I.

Binding and signaling properties of tagged KISS1R were determined to ensure preservation of receptor function. Displacement of ^{125}I-kisspeptin by increasing unlabeled kisspeptin was not affected by the addition of MYC- (Fig. 3A) or CFP- (Fig. 3C) tags, indicating that neither affinity to kisspeptin nor maximal binding capacity were affected by these tags. Likewise, ability of MYC- or CFP-KISS1R to activate G protein signaling was preserved in the tagged KISS1R, as shown by kisspeptin-stimulated inositol phosphate accumulation in cells expressing the tagged receptors (Fig. 3, B and D). While inositol phosphate production by the MYC-KISS1R was comparable to that of the untagged WT KISS1R (Fig. 3B), the addition of
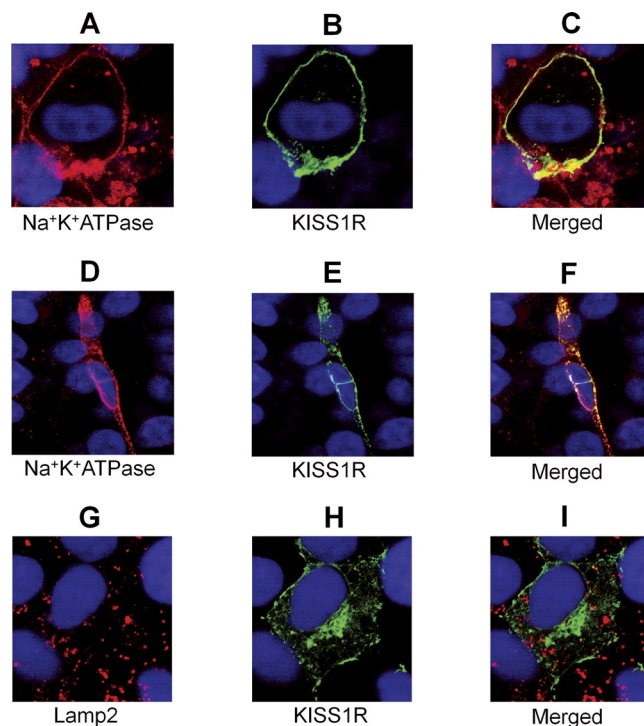

FIG. 2. Subcellular localization of KISS1R by confocal microscopy. COS-7 cells expressing MYC-KISS1R (Na$^+$K$^+$ATPase colocalization) or CFP-KISS1R (Lamp2 colocalization) were stimulated with 10^{-7} M kisspeptin for 0–5 h. Anti-CFP antibody was conjugated to FITC (*green*), whereas membrane (Na$^+$K$^+$ATPase) and lysosome (Lamp2) markers were visualized by Alexa-568-conjugated antibodies (*red*). Na$^+$K$^+$ATPase (A), KISS1R at baseline (B), and the merged (A + B) image (C); Na$^+$K$^+$ATPase (D), KISS1R after 3 h of kisspeptin stimulation (E), and the merged (D + E) image (F); Lamp2 (G), KISS1R at baseline (H), and the merged (G + H) image (I). Note: D–F, Featured cell is in an upper confocal plan when compared with others. Nuclei are shown in *blue* (DAPI). Magnification of the images is indicated by the *white bar* (scale, 20 μM).

the CFP-tag slightly reduced the response of CFP-KISS1R to kisspeptin stimulation (Fig. 3D). Such an effect has been observed for other GPCRs after the addition of fluorescent tags (23). Nonetheless, fusion of fluorescent tags to GPCRs is widely used and considered a powerful tool in GPCR imaging (24).

KISS1R protein levels are increased in the presence of an inhibitor of proteasome degradation

Representative Western-blots in Fig. 4, A and B show a potential involvement of the proteasome in KISS1R degradation. The first five lanes of Fig. 4, A (COS-7 cells) and B (HEK-293 cells) were loaded with immunocomplexes precipitated with an anti-myc antibody, whereas lanes 6 through 10 were loaded with the corresponding whole cell lysates. HEK-293 cells have been reported recently to express KISS1R endogenously (20) and thus are physiologically relevant. MYC-KISS1R monomer was detected in all lanes except for 1 and 6, which were transfected with control vector alone. In addition, nonspecific bands detected in whole cell lysates of cells expressing control vec-
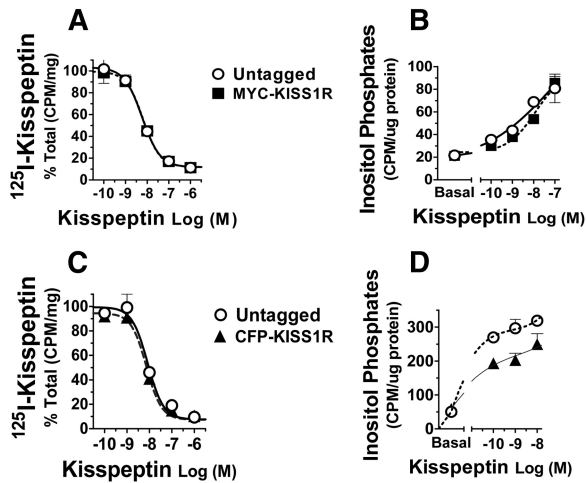
FIG. 3. Binding and signaling by tagged KISS1R. A and C, Binding displacement assay of MYC- (A) and CFP- (C) KISS1R. COS-7 cells expressing untagged or tagged KISS1R were incubated with ^{125}I-kisspeptin alone or in the presence of increasing concentrations (10^{-10} to 10^{-6} M) of unlabeled kisspeptin. Results are the mean ± SE of triplicate samples from a representative experiment and are shown as percentage of maximal binding (*i.e.*, binding in the absence of unlabeled kisspeptin). Experiments were repeated at least three times with similar results. B and D, Total inositol phosphate production by MYC- (B) or CFP- (D) KISS1R. Cells expressing untagged or tagged KISS1R were stimulated with increasing kisspeptin concentrations (10^{-10} to 10^{-7} M) for 2 h at 37 C. Results are the mean ± SE of triplicates from a representative experiment. Experiments were repeated at least three times with similar results. *Open circles*, untagged KISS1R; *squares*, MYC-KISS1R; *triangles*, CFP-KISS1R.
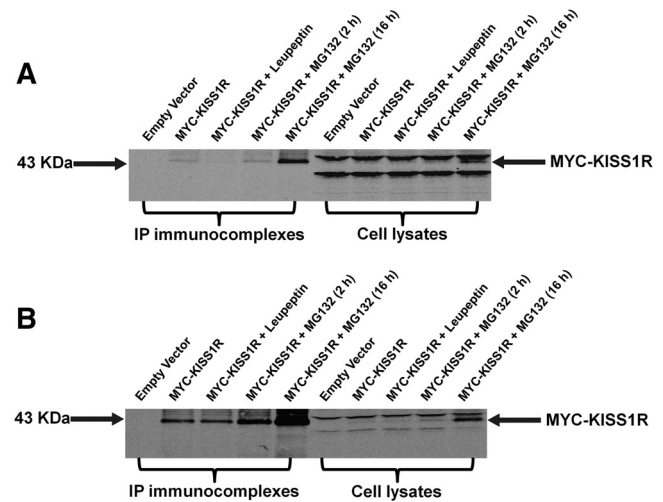

FIG. 4. Western-Blot detection of MYC-KISS1R. COS-7 (A) or HEK-293 (B) cells expressing MYC-KISS1R were incubated at 37 C with or without leupeptin (lysosome inhibitor) for 16 h or with MG132 (proteasome inhibitor) for 2 h or 16 h before lysis. Cell lysates underwent immunoprecipitation (IP) with a monoclonal anti-myc antibody followed by Western blot analysis. MYC-KISS1R in whole cell lysates or anti-myc immunoprecipitants was detected using a polyclonal anti-myc antibody (1:1,000) followed by a fluorescent-labeled infrared dye IRDye-800CW-conjugated antirabbit antibody (1:5,000). Lanes 1 through 5 were loaded with immunoprecipitated complexes, and lanes 6 through 10 with the corresponding pre-IP whole cell lysates. Lanes 1 and 6, control vector; lanes 2 and 7, MYC-KISS1R alone; Lanes 3 and 8, MYC-KISS1R + Leupeptin (16 h); lanes 4 and 9, MYC-KISS1R + MG132 (2 h); lanes 5 and 10, MYC-KISS1R + MG132 (16 h). Arrow on the right points to KISS1R monomers at 43 kDa. Western blot of representative experiments are shown. Experiments were repeated at least three times with comparable results.

tor were eliminated by immunoprecipitation (*i.e.*, lane 6 *vs.* lane 1 of Fig. 4, A and B). Lanes 3 and 8 of both Western blots show that overnight incubation with leupeptin, a lysosome inhibitor, did not affect KISS1R levels in COS-7 (Fig. 4A) or HEK-293 (Fig. 4B) cells, indicating that lysosome degradation of KISS1R is low or absent. Conversely, overnight incubation with MG132, a proteasome uptake inhibitor, markedly increased KISS1R in COS-7 cells (lane 5 *vs.* lane 2, Fig. 4A). This effect was even stronger in HEK-293 cells (lane 5 *vs.* lane 2, Fig. 4B). These results suggest proteasomal degradation of KISS1R.

Rate of KISS1R trafficking is not affected by the Arg386Pro mutation

Internalization is involved in the desensitization of many GPCRs (15). Accordingly, our initial hypothesis was that the Arg386Pro mutation would reduce internalization or increase recycling of KISS1R, thereby prolonging responsiveness to kisspeptin. This hypothesis was tested *in vitro* by comparing the rate of trafficking (internalization/recycling) of the Arg386Pro mutant to that of WT KISS1R under the same conditions. This rate measures the relative percentile distribution of receptors in membrane and internalized fractions at specific time points. Binding of ^{125}I-kisspeptin was used to detect and track receptors in both fractions. Results in Fig. 5A show

that the rate of KISS1R trafficking was not affected by the Arg386Pro mutation, as indicated by a comparable time-dependent decrease in the relative distribution of membrane receptors (Fig. 5A, left panel) for the WT (open bars) and mutant (closed bars) KISS1R. The relative membrane decay of both receptors correlated well with proportional increases in the relative internalized receptors (Fig. 5A, right panel), indicating that WT and Arg386Pro KISS1R internalize and recycle at similar rates. About 60% of both receptors were internalized after 30 min of stimulation (58% and 57% for WT and Arg386Pro KISS1R, respectively), whereas 42% of WT and 43% of Arg386Pro KISS1R remained on the cell surface. At 120 min, about 75% of both receptors were internalized (75% and 74% for WT and Arg386Pro KISS1R, respectively), whereas the remaining (25% of WT and 26% of mutant KISS1R) localized to the cell surface. Thus, contrary to our initial expectations, changes in receptor internalization/ recycling are not responsible for the delayed desensitization/ increased responsiveness of Arg386Pro KISS1R mutant to kisspeptin.

On the other hand, the absolute number of total Arg386Pro KISS1R was significantly increased after 120 min of stimulation compared with WT KISS1R, despite
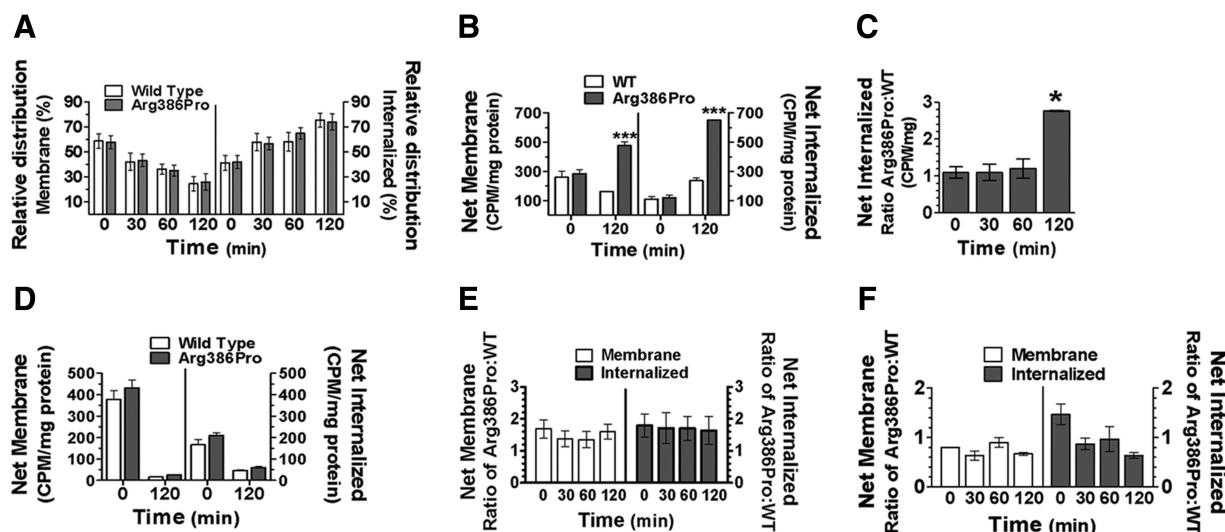
FIG. 5. Membrane trafficking of KISS1R. COS-7 cells expressing wild-type (WT) or Arg386Pro KISS1R were equilibrated with ^{125}I-kisspeptin on ice before incubation at 37 C for 0–120 min as indicated. Membrane and internalized ^{125}I-kisspeptin were extracted and counted as described in the *Materials and Methods*. A, Rate of membrane trafficking (internalization and recycling) in WT and Arg386Pro KISS1R is represented as the relative distribution of receptors in the membrane and internalized at each time-point. *Left panel*, relative percent of receptor in the membrane; *right panel*, relative percent of internalized receptors. Results are the mean ± SE of seven independent experiments. *Open bars*, WT KISS1R; *solid bars*, Arg386Pro KISS1R. B, Total KISS1R trafficking with detection of recycled receptors. Total receptors in membrane (*left panel*) or internalized (*right panel*) fractions are shown as cpm/mg protein of the mean ± SE of triplicates in this representative experiment, which was repeated at least three times with comparable results. *Open bars*, WT KISS1R; *solid bars*, Arg386Pro KISS1R. ***, $P < 0.0002$ by Student's *t* test *vs.* WT receptor at 120 min. C, Ratio of (total) internalized KISS1R with detection of recycled receptors: Time-course of stimulation. Bars represent the combined ratio derived from three independent experiments. Ratio in each experiment was calculated by dividing the mean of triplicate measurements of Arg386Pro KISS1R by that of triplicate measurements from WT receptor. *, $P < 0.05$ by ANOVA followed by the Dunnett's test *vs.* time zero. D and E, Measurement of KISS1R trafficking without detection of recycled receptors: Effect of removal of radioligand. In D and E, unbound ^{125}I-kisspeptin was removed at the end of equilibration on ice but before incubation at 37 C, so that only receptors bound to radioligand at time zero could be detected and tracked thereafter. D, The (total) receptors are represented as the mean ± SE of triplicate samples from a representative experiment shown as cpm/mg of protein, replicated at least three times with comparable results. *Open bars*, WT KISS1R; *solid bars*, Arg386Pro KISS1R. *Left panel*, total membrane receptors; *right panel*, total internalized receptors. E, Combined ratio of Arg386Pro:WT KISS1R. Bars represent the average ratio derived from three independent time-course experiments. The ratio of each experiment was calculated by dividing the mean of triplicate samples of Arg386Pro KISS1R by that of triplicate samples of WT KISS1R from the same experiment. *Left panel* (*open bars*), ratio in the membrane; *right panel* (*solid bars*), ratio of internalized receptors. F, KISS1R trafficking without detection of recycled receptors: Effect of pretreatment with monensin. Thirty minutes of incubation with monensin (recycling inhibitor) before the addition of ^{125}I-kisspeptin prevented the reinsertion of recycled receptors into the membrane. Results are the mean ± SE of triplicate samples from a representative experiment, shown as the ratio of Arg386Pro over WT KISS1R. *Left panel* (*open bars*), ratio in the membrane; *right panel* (*solid bars*), ratio of internalized receptors.

there being a similar number of receptors present at baseline (Fig. 5, B and C). As opposed to the decline in the absolute amount in the membrane, as observed for the WT receptor after 120 min, the Arg386Pro KISS1R displayed a 3-fold increase in membrane receptors (Fig. 5B, left panel) at the same time point. This finding is consistent with results we previously reported (12). Also, an increase of similar magnitude was observed for this mutant compared with WT KISS1R in internalized receptors after 120 min of stimulation (Fig. 5B, right panel and combined results in Fig. 5C). The time required for the detection of these differences demonstrates that this mutant affects long-term KISS1R desensitization.

Increased total measured binding to Arg386Pro KISS1R is eliminated by blocking detection of recycled receptors

To further investigate the effect of the Arg386Pro mutation on long-term KISS1R desensitization, detection of

[125]I-kisspeptin binding to recycled receptors was blocked by removal of unbound radioligand after equilibration. Thus, by preventing the subsequent binding of ^{125}I-kisspeptin to recycled receptors, only receptors bound to radioligand at baseline (*i.e.*, after equilibration on ice but before incubation at 37 C) would be detected and tracked thereafter. Although this approach does not prevent reinsertion of recycled receptors into the membrane, these receptors are no longer detected. Interestingly, this approach completely eliminated the previously observed increases of Arg386Pro KISS1R in both the membrane and internalized fractions (Fig. 5, D and E), indicating that newly recycled receptors account for the increases in total Arg386Pro KISS1R compared with WT KISS1R.

Similar results with comparable elimination of the increases in Arg386Pro compared with WT KISS1R were observed using an alternative approach in which pretreat-

ment with monensin prevented membrane reinsertion of recycled receptors (Fig. 5F). This approach provides further confirmation that recycling of KISS1R accounts for the stimulation-dependent increases in total Arg386Pro KISS1R over time. In addition, the 2-h frame required for detection of this effect indicates involvement of long-term desensitization of KISS1R. This, in turn, suggests slower degradation of the mutant KISS1R, because long-term desensitization is accomplished by receptor degradation (18).

Another interesting consequence of the blockage of detection of recycled receptors is the considerable decrease in total receptors after 120 min of stimulation. As opposed to the ~3-fold increase in total mutant receptors in the membrane (Fig. 5B, left panel) and internalized (Fig. 5B, right panel) after 120 min with detection of recycled receptors, blockade of detection of recycled receptors resulted in a ~20-fold decrease in mutant, as well as wild-type receptors on the membrane (Fig. 5D, left panel) and a ~4-fold decrease in intracellular receptors (Fig. 5D, left panel) for both wild-type and mutant KISS1R. This finding demonstrates that a substantial amount of receptors detected in both membrane and internalized fractions correspond to recycled receptors, thereby suggesting that recycled receptors are responsible for a considerable portion of KISS1R signaling.

Discussion

Heritable factors are responsible for 70–80% of the variability in the timing of puberty (25, 26). Despite this unquestionable genetic component, the precise mechanisms regulating pubertal maturation and the genetic causes underlying the majority of cases of pubertal disorders remain unknown. The identification and functional characterization of mutations identified in patients with pubertal disorders has been the main source of insights into the mechanisms that initiate puberty (27–29). A subset of patients with reproductive disorders have mutations in the KISS1R, some of which have been characterized *in vitro* (30). All but one of the amino acid substitutions in KISS1R that have been characterized are inactivating mutations that were shown or predicted to impair receptor function (8–11, 31). The impaired signaling of inactive mutants limits the utility of these mutants to characterize the physiological regulation of KISS1R signaling. On the other hand, the gain-of-function effect of the Arg386Pro mutation has proven to serve as a useful model to study KISS1R desensitization. To understand how this mutation enhances KISS1R signaling to contribute to the precocious puberty phenotype, we investigated the effect of this mutation on KISS1R trafficking and turnover.

A time-dependent desensitization (despite continuous presence of ligand) that culminates with complete suppression of signaling is the typical response of KISS1R to activation by ligand. This phenomenon is depicted in Fig. 1A, which reinforces and further explains previous findings describing desensitization of physiological responses upon continuous kisspeptin stimulation *in vivo*, such as those in agonadal monkeys (16) and female (13) and male (14) rats. These observations emphasize the key role of regulation of KISS1R signaling and desensitization in the control of pubertal development and maintenance of reproductive capability, as well as in clinical disorders caused by disturbances of KISS1R desensitization.

As described for other GPCRs, results presented here demonstrate that ligand-induced desensitization of KISS1R involves time-dependent internalization (Fig. 1B), which confirms and further characterizes a recent report of ligand-induced internalization of KISS1R in HEK-293 cells (20) and indicates that this effect is not cell-specific. A percentage of internalized GPCR is recycled back to the membrane, whereas the remaining is degraded (18). Although the proportions of recycled/degraded GPCRs may vary considerably among receptors, persistent activation of the majority of GPCRs will eventually lead to long-term desensitization attributable to receptor degradation. Internalized receptor fate is subject to endogenous regulation and the same GPCR may undergo desensitization by more than one pathway (18, 32, 33). Here, we used biochemical techniques such as radioligand binding, immunoprecipitation, and immunofluorescence imaging to investigate the pathway of KISS1R degradation, as well as the effect of the Arg386Pro mutation on the timeline of long-term desensitization of KISS1R.

Small tags, such as MYC, are not expected to affect receptor function, whereas large fluorescent tags such as CFP may affect function, yet preserving the ability of the receptor to signal, as described for the β-2 adrenergic receptor (34), the α-1 adrenergic receptor (35), and the cholecystokinin receptor (36). These predicted behaviors were observed for the MYC- (Fig. 3, A and C) and CFP-KISS1R (Fig. 3, B and D) used here. Persistent membrane localization of KISS1R was detected at baseline and at a variety of time points after kisspeptin stimulation. Representative images in Fig. 2 show membrane localization at baseline (Fig. 2, A–C) and after 3 h of stimulation with a high concentration (10^{-7} M) of kisspeptin (Fig. 2, D–F), suggesting that internalized KISS1R is sorted for recycling rather than degradation. Nevertheless, internalization was noticeable at all time points of stimulation with no noticeable differences in the relative percentage of internalized receptors from 5 min to 5 h of stimulation. About 25% of receptors were internalized at the representative

time point shown in Fig. 2, D–F. However, these images are not intended to be quantitative and this percentage variation is an estimation.

No colocalization with a lysosome marker was detected after up to 5 h of stimulation with the same high concentration of kisspeptin. The ~40% decay in inositol phosphate accumulation after 4 h of stimulation with 100-fold lower concentration of kisspeptin (10^{-9} M) in Fig. 1A indicates desensitization of Gq signaling at this time point. Therefore, a more extensive degree of desensitization would be predicted after 5 h of stimulation with a higher concentration of kisspeptin. By this point, receptor degradation is expected and should be detected (37). Thus, absence of colocalization with lysosomes after 5 h of stimulation suggests that lysosomal degradation of KISS1R is low or absent.

Degradation by lysosomes is the major pathway of GPCR destruction (38). Accordingly, colocalization of GPCRs with lysosomal markers has been detected as soon as 5 min (37) and up to 6 h (39, 40) after exposure to ligand. Lack of colocalization of Lamp2 with KISS1R suggests that lysosomes may not be the preferential degradation pathway of KISS1R. This was confirmed by the lack of effect of the lysosome inhibitor on the levels of KISS1R protein after 16 h incubation in both COS-7 and HEK-293 cells (Fig. 4, A and B). On the other hand, overnight treatment of the same cells with a proteasome inhibitor led to substantial increases in KISS1R protein in both cell lines (Fig. 4, A and B), indicating proteasome degradation of KISS1R. Detection of this effect in HEK-293 cells is especially relevant because these cells express KISS1R endogenously (20). Although less common, proteasome degradation has been reported for some GPCRs such as the opioid (41) and β-adrenergic receptors (42).

The dynamic trafficking of KISS1R suggested by immunofluorescence was confirmed by KISS1R trafficking (internalization/recycling) studies. Prevention of detection of recycling largely decreased total membrane (Fig. 5D, left panel) and internalized (Fig. 5D, right panel) KISS1R detected after 120 min of stimulation. This finding demonstrates that dynamic recycling provides for a considerable amount of binding and signaling of KISS1R upon kisspeptin stimulation. Thus, KISS1R recycling is physiologically relevant. Additionally, disturbances of this dynamic cycling may significantly affect overall KISS1R signaling. Interestingly, our results show that the Arg386Pro mutation associated with central precocious puberty alters KISS1R trafficking. Despite displaying equivalent binding at baseline, the Arg386Pro mutant was significantly increased compared with WT KISS1R after 120 min of stimulation with ^{125}I-kisspeptin (Fig. 5B). This effect is likely contributing to the slower desensitization of inositol

phosphate accumulation and ERK phosphorylation in response to kisspeptin by this mutant (12).

KISS1R was reported to undergo rapid ligand-induced internalization, as well as colocalize with arrestin (20), which binds phosphorylated receptors (43, 44) preventing further G protein–coupling and triggering receptor internalization (45, 46). Accordingly, a reduced rate of internalization (or increased rate of recycling) was initially presumed to account for the slower rate of desensitization of the Arg386Pro mutant. However, the relative rate of KISS1R trafficking is not affected by the Arg385Pro mutation (Fig. 5A), as indicated by similar relative distribution of WT and mutant receptors in the membrane and internalized at baseline and at all subsequent time points after stimulation (Fig. 5A). Therefore, the event affected by the Arg386Pro mutation is downstream of receptor internalization. Additionally, unaltered KISS1R trafficking eliminates the potential involvement of arrestin-mediated internalization on the effect of the Arg386Pro mutation. On the other hand, degradation is downstream of internalization, leads to reduced membrane receptors and loss of binding, and is characteristic of long-term GPCR desensitization (18, 38). All of these features match effects of the Arg386Pro mutation. In fact, effects of this mutation are only detected when membrane KISS1R binding and signaling are declining.

In contrast, the dynamic trafficking is preserved in the Arg386Pro mutant, as indicated by the unaltered relative distribution of mutant KISS1R in membrane and internalized fractions, as well as by the same substantial decrease in mutant receptors when detection of recycled receptors is prevented (Fig. 5, D–F). Of note, the substantial decrease in membrane binding also indicates that receptor recycling is responsible for a great deal of KISS1R signaling. Hence, the combination of dynamic trafficking with decreased degradation is likely responsible for the overall slower loss of binding and signaling by this mutant, thereby prolonging responsiveness of Arg386Pro KISS1R to kisspeptin (12) in the absence of changes in the rate of receptor trafficking.

A proposed model of KISS1R trafficking as well as the effect of the Arg386Pro mutation on KISS1R trafficking after 120 min of stimulation is depicted in Fig. 6. According to this model, which displays data from Figure 5B, a similar number of WT and Arg386Pro KISS1R are detected in the membrane (7 receptors) and internalized (3 receptors) fractions of cells expressing WT (top left) or Arg386Pro (bottom left) under basal conditions (baseline). Accordingly, the relative distribution of these receptors at baseline is equally similar: 70% in the membrane and 30% internalized for WT (top left) and Arg386Pro KISS1R (bottom left). After 120 min of stimulation, rel-
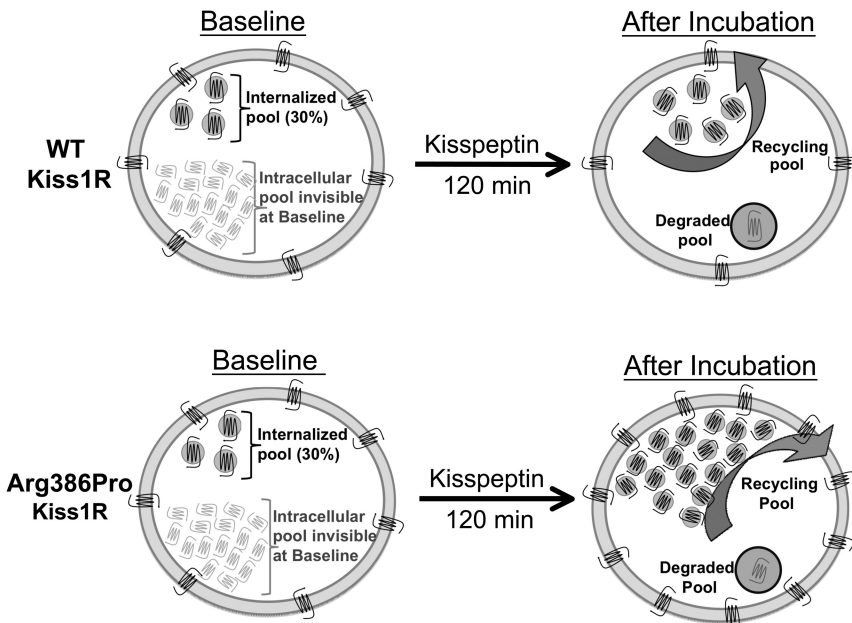
FIG. 6. Proposed model of KISS1R trafficking and effect of the Arg386Pro mutation. Under basal conditions, a similar number of receptors is detected on the membrane (seven receptors) and internalized (three receptors) fractions in cells expressing WT (*top left*) or Arg386Pro (*bottom left*) KISS1R. Relative distribution at baseline is also similar: 70% on the membrane and 30% internalized for both WT (*top left*) and Arg386Pro (*bottom left*) KISS1R. After 120 min of stimulation, relative distribution remains similar for WT (*top right*) and Arg386Pro (*bottom right*) KISS1R: 40% on the membrane and 60% internalized. However, total receptor number is no longer similar. WT KISS1R decreased to 4 on the membrane and increased to 6 internalized (*top right*), whereas Arg386Pro KISS1R increased on both fractions after stimulation: 11 on the membrane and 17 internalized (*bottom right*). A small percentage of receptors is degraded after internalization, and a reduced rate of degradation of Arg386Pro KISS1R is proposed to increase intracellular accumulation of this mutant, which combined to a dynamic recycling would be enough to account for the time-dependent magnification of kisspeptin responsiveness by this mutant. A pool of intracellular KISS1R not initially detected at baseline (in *gray*) is proposed to be recruited to the membrane and thus account for the apparent increases in receptor number after stimulation. Values on this figure are based on data represented in Fig. 5B.

ative distribution remains similar, with 40% in the membrane and 60% internalized for WT (top right) and Arg386Pro KISS1R (bottom right). However, absolute number of receptors is no longer similar. Net Arg386Pro receptors (11 in the membrane and 17 internalized; bottom right) are increased when compared with WT receptors (4 in the membrane and 6 internalized; top right). Reduced degradation of mutant KISS1R is proposed to account for this increase by leading to intracellular accumulation of this mutant. Combination of intracellular accumulation with a dynamic recycling of the Arg386Pro KISS1R results in the magnification of kisspeptin responsiveness after 120 min by this mutant compared with WT receptor. An additional pool of intracellular KISS1R not initially detected at baseline (shown in gray on Fig. 6) is proposed to be recruited to the membrane and account for the apparent increases in mutant receptor number after stimulation.

Decreased receptor degradation was reported as the mechanism underlying a gain-of-function mutation of another GPCR (47). In this report, lysosomal degradation of

LH receptor is blocked by a mutation that generates a constitutively active LH receptor. This receptor escapes degradation, which leads to a marked increase in signaling at baseline. As opposed to this constitutively active LH receptor that does not require the presence of ligand to activate signaling (47), effects of the Arg386Pro KISS1R can only be detected during ligand-induced receptor desensitization, which indicates a requirement for ligand activation of the receptor. This distinctive feature allows for endogenous regulation of the activity of Arg386Pro KISS1R, which has implications for the overall phenotype of the patient carrying this mutation. As opposed to the constitutive activation of the LH receptor that results in gonadotropin-independent precocious puberty, persistent central activation of the reproductive axis produces the opposite effect. Evidence of this is the therapeutic use of GnRH agonists to suppress the activity of the reproductive axis in patients with gonadotropin-dependent precocious puberty. Mimicking the effect of constitutively active mutants, GnRH agonists efficiently suppress the activity of the axis after transitory activation.

Functional characterization of a mutation in kisspeptin (Pro74Ser) also associated with precocious puberty revealed increased inositol phosphate accumulation after preincubation of this mutant with human serum compared with wild-type kisspeptin under the same conditions. This suggests that this mutation increases kisspeptin stability thereby prolonging signaling and contributing to the precocious puberty phenotype of the boy carrying the mutation (48). Therefore, functionally characterized mutations associated with central precocious puberty suggest that duration of KISS1R stimulation, signaling, and desensitization are crucial for the role of this receptor/ligand system in timing the onset of puberty. Thus, mutations in other (yet unknown) proteins that would result in dysregulation of KISS1R signaling, trafficking, recycling, or degradation may be responsible for other cases of precocious puberty (and potentially other reproductive abnormalities) yet unexplained. This underscores the importance of a detailed characterization of pathways involved that will help in the understanding, diagnosis, and treatment of such cases.

Additional mutations have been identified in a screen for polymorphisms in KISS1R or kisspeptin in Chinese females with central precocious puberty. A KISS1R mutation (Pro196His) located in the second extracellular loop of the receptor was identified (49), as was a kisspeptin variant (Pro110Thr). No functional studies have been performed for either mutation, so the mechanism by which these mutations might be associated with precocious puberty remains to be elucidated (49, 50).

To our knowledge, this is the first study investigating KISS1R degradation pathway, as well as the first description of the dynamic membrane trafficking of the KISS1R. These findings open up new roads for the investigation of mutations affecting KISS1R activity.

Acknowledgments

References

1. Gottsch ML, Cunningham MJ, Smith JT, Popa SM, Acohido BV, Crowley WF, Seminara S, Clifton DK, Steiner RA 2004 A role for kisspeptins in the regulation of gonadotropin secretion in the mouse. Endocrinology 145:4073–4077

2. Irwig MS, Fraley GS, Smith JT, Acohido BV, Popa SM, Cunningham MJ, Gottsch ML, Clifton DK, Steiner RA 2004 Kisspeptin activation of gonadotropin releasing hormone neurons and regulation of KiSS-1 mRNA in the male rat. Neuroendocrinology 80:264–272

3. Matsui H, Takatsu Y, Kumano S, Matsumoto H, Ohtaki T 2004 Peripheral administration of metastin induces marked gonadotropin release and ovulation in the rat. Biochem Biophys Res Commun 320:383–388

4. Navarro VM, Castellano JM, Fernandez-Fernandez R, Barreiro ML, Roa J, Sanchez-Criado JE, Aguilar E, Dieguez C, Pinilla L, Tena-Sempere M 2004 Developmental and hormonally regulated messenger ribonucleic acid expression of KiSS-1 and its putative receptor, GPR54, in rat hypothalamus and potent luteinizing hormone-releasing activity of KiSS-1 peptide. Endocrinology 145:4565–4574

5. Shahab M, Mastronardi C, Seminara SB, Crowley WF, Ojeda SR, Plant TM 2005 Increased hypothalamic GPR54 signaling: a potential mechanism for initiation of puberty in primates. Proc Natl Acad Sci USA 102:2129–2134

6. Messager S, Chatzidaki EE, Ma D, Hendrick AG, Zahn D, Dixon J, Thresher RR, Malinge I, Lomet D, Carlton MB, Colledge WH, Caraty A, Aparicio SA 2005 Kisspeptin directly stimulates gonadotropin-releasing hormone release via G protein-coupled receptor 54. Proc Natl Acad Sci USA 102:1761–1766

7. Vogel G 2005 Reproductive biology. A powerful first KiSS-1. Science 309:551–552

8. de Roux N, Genin E, Carel JC, Matsuda F, Chaussain JL, Milgrom E 2003 Hypogonadotropic hypogonadism due to loss of function of the KiSS1-derived peptide receptor GPR54. Proc Natl Acad Sci USA 100:10972–10976

9. Seminara SB, Messager S, Chatzidaki EE, Thresher RR, Acierno Jr JS, Shagoury JK, Bo-Abbas Y, Kuohung W, Schwinof KM, Hendrick AG, Zahn D, Dixon J, Kaiser UB, Slaugenhaupt SA, Gusella JF, O'Rahilly S, Carlton MB, Crowley Jr WF, Aparicio SA, Colledge WH 2003 The GPR54 gene as a regulator of puberty. N Engl J Med 349:1614–1627

10. Semple RK, Achermann JC, Ellery J, Farooqi IS, Karet FE, Stanhope RG, O'Rahilly S, Aparicio SA 2005 Two novel missense mutations in g protein-coupled receptor 54 in a patient with hypogonadotropic hypogonadism. J Clin Endocrinol Metab 90:1849–1855

11. Tenenbaum-Rakover Y, Commenges-Ducos M, Iovane A, Aumas C, Admoni O, de Roux N 2007 Neuroendocrine phenotype analysis in five patients with isolated hypogonadotropic hypogonadism due to a L102P inactivating mutation of GPR54. J Clin Endocrinol Metab 92:1137–1144

12. Teles MG, Bianco SD, Brito VN, Trarbach EB, Kuohung W, Xu S, Seminara SB, Mendonca BB, Kaiser UB, Latronico AC 2008 A GPR54-activating mutation in a patient with central precocious puberty. N Engl J Med 358:709–715

13. Roa J, Vigo E, Garcia-Galiano D, Castellano JM, Navarro VM, Pineda R, Dieguez C, Aguilar E, Pinilla L, Tena-Sempere M 2008 Desensitization of gonadotropin responses to kisspeptin in the female rat: analyses of LH and FSH secretion at different developmental and metabolic states. Am J Physiol Endocrinol Metab 294:E1088–E1096

14. Thompson EL, Murphy KG, Patterson M, Bewick GA, Stamp GW, Curtis AE, Cooke JH, Jethwa PH, Todd JF, Ghatei MA, Bloom SR 2006 Chronic subcutaneous administration of kisspeptin-54 causes testicular degeneration in adult male rats. Am J Physiol Endocrinol Metab 291:E1074–E1082

15. Lefkowitz RJ 1998 G protein-coupled receptors. III. New roles for receptor kinases and β-arrestins in receptor signaling and desensitization. J Biol Chem 273:18677–18680

16. Seminara SB, Dipietro MJ, Ramaswamy S, Crowley Jr WF, Plant TM 2006 Continuous human metastin 45–54 infusion desensitizes G protein–coupled receptor 54-induced gonadotropin-releasing hormone release monitored indirectly in the juvenile male Rhesus monkey (Macaca mulatta): a finding with therapeutic implications. Endocrinology 147:2122–2126

17. Ritter SL, Hall RA 2009 Fine-tuning of GPCR activity by receptor-interacting proteins. Nat Rev Mol Cell Biol 10:819–830

18. Ferguson SS 2001 Evolving concepts in G protein-coupled receptor endocytosis: the role in receptor desensitization and signaling. Pharmacol Rev 53:1–24

19. Xu ZQ, Zhang X, Scott L 2007 Regulation of G protein-coupled receptor trafficking. Acta Physiol (Oxf) 190:39–45

20. Pampillo M, Camuso N, Taylor JE, Szereszewski JM, Ahow MR, Zajac M, Millar RP, Bhattacharya M, Babwah AV 2009 Regulation of GPR54 signaling by GRK2 and β-arrestin. Mol Endocrinol 23:2060–2074

21. Sagar GD, Gereben B, Callebaut I, Mornon JP, Zeold A, da Silva WS, Luongo C, Dentice M, Tente SM, Freitas BC, Harney JW, Zavacki AM, Bianco AC 2007 Ubiquitination-induced conforma-

tional change within the deiodinase dimer is a switch regulating enzyme activity. Mol Cell Biol 27:4774–4783

22. **Kuohung W, Burnett M, Mukhtyar D, Schuman E, Ni J, Crowley WF, Glicksman MA, Kaiser UB** *In press* A high-throughput small-molecule ligand screen targeted to agonists and antagonists of the G-protein-coupled receptor GPR54. J Biomol Screen 15:508–517.

23. **Perret BG, Wagner R, Lecat S, Brillet K, Rabut G, Bucher B, Pattus F** 2003 Expression of EGFP-amino-tagged human mu opioid receptor in Drosophila Schneider 2 cells: a potential expression system for large-scale production of G-protein coupled receptors. Protein Expr Purif 31:123–132

24. **Balla T** 2009 Green light to illuminate signal transduction events. Trends Cell Biol 19:575–586

25. **Palmert MR, Boepple PA** 2001 Variation in the timing of puberty: clinical spectrum and genetic investigation. J Clin Endocrinol Metab 86:2364–2368

26. **Palmert MR, Hirschhorn JN** 2003 Genetic approaches to stature, pubertal timing, and other complex traits. Mol Genet Metab 80: 1–10

27. **Iovane A, Aumas C, de Roux N** 2004 New insights in the genetics of isolated hypogonadotropic hypogonadism. Eur J Endocrinol 151(Suppl 3):U83–U88

28. **Trarbach EB, Silveira LG, Latronico AC** 2007 Genetic insights into human isolated gonadotropin deficiency. Pituitary 10:381–391

29. **Chan YM, Broder-Fingert S, Seminara SB** 2009 Reproductive functions of kisspeptin and Gpr54 across the life cycle of mice and men. Peptides 30:42–48

30. **Bianco SD, Kaiser UB** 2009 The genetic and molecular basis of idiopathic hypogonadotropic hypogonadism. Nat Rev Endocrinol 5:569–576

31. **Teles M, Trarbach E, Sekoni N, Guerra-Junior G, Jorge A, Beneduzzi D, Bianco S, Mukherjee A, Baptista MT, Costa E, De Castro M, de Mendonca B, Kaiser U, Latronico AC** 2010 A novel homozygous splice acceptor site mutation of KISS1R in two siblings with normosmic isolated hypogonadotropic hypogonadism. Eur J Endocrinol 163:29–34

32. **Gurevich VV, Gurevich EV** 2006 The structural basis of arrestin-mediated regulation of G-protein-coupled receptors. Pharmacol Ther 110:465–502

33. **Blaukat A, Pizard A, Breit A, Wernstedt C, Alhenc-Gelas F, Muller-Esterl W, Dikic I** 2001 Determination of bradykinin B2 receptor in vivo phosphorylation sites and their role in receptor function. J Biol Chem 276:40431–40440

34. **Barak LS, Ferguson SS, Zhang J, Martenson C, Meyer T, Caron MG** 1997 Internal trafficking and surface mobility of a functionally intact β2-adrenergic receptor-green fluorescent protein conjugate. Mol Pharmacol 51:177–184

35. **Hirasawa A, Sugawara T, Awaji T, Tsumaya K, Ito H, Tsujimoto G** 1997 Subtype-specific differences in subcellular localization of α1-adrenoceptors: chlorethylclonidine preferentially alkylates the accessible cell surface α1-adrenoceptors irrespective of the subtype. Mol Pharmacol 52:764–770

36. **Tarasova NI, Stauber RH, Choi JK, Hudson EA, Czerwinski G,** Miller JL, Pavlakis GN, Michejda CJ, Wank SA 1997 Visualization of G protein-coupled receptor trafficking with the aid of the green fluorescent protein. Endocytosis and recycling of cholecystokinin receptor type A. J Biol Chem 272:14817–14824

37. **Moore RH, Tuffaha A, Millman EE, Dai W, Hall HS, Dickey BF, Knoll BJ** 1999 Agonist-induced sorting of human β2-adrenergic receptors to lysosomes during downregulation. J Cell Sci 112:329–338.

38. **Hanyaloglu AC, von Zastrow M** 2008 Regulation of GPCRs by endocytic membrane trafficking and its potential implications. Annu Rev Pharmacol Toxicol 48:537–568

39. **Mosser VA, Jones KT, Hoffman KM, McCarty NA, Jackson DA** 2008 Differential role of β-arrestin ubiquitination in agonist-promoted down-regulation of M1 vs M2 muscarinic acetylcholine receptors. J Mol Signal 3:20

40. **Rocca A, Lamaze C, Subtil A, Dautry-Varsat A** 2001 Involvement of the ubiquitin/proteasome system in sorting of the interleukin 2 receptor β chain to late endocytic compartments. Mol Biol Cell 12:1293–1301

41. **Chaturvedi K, Bandari P, Chinen N, Howells RD** 2001 Proteasome involvement in agonist-induced down-regulation of mu and delta opioid receptors. J Biol Chem 276:12345–12355

42. **Shenoy SK, McDonald PH, Kohout TA, Lefkowitz RJ** 2001 Regulation of receptor fate by ubiquitination of activated β 2-adrenergic receptor and β-arrestin. Science 294:1307–1313

43. **Palczewski K, Buczylko J, Kaplan MW, Polans AS, Crabb JW** 1991 Mechanism of rhodopsin kinase activation. J Biol Chem 266:12949–12955

44. **Gurevich VV, Benovic JL** 1993 Visual arrestin interaction with rhodopsin. Sequential multisite binding ensures strict selectivity toward light-activated phosphorylated rhodopsin. J Biol Chem 268:11628–11638

45. **Krupnick JG, Gurevich VV, Benovic JL** 1997 Mechanism of quenching of phototransduction. Binding competition between arrestin and transducin for phosphorhodopsin. J Biol Chem 272:18125–18131

46. **Drake MT, Shenoy SK, Lefkowitz RJ** 2006 Trafficking of G protein-coupled receptors. Circ Res 99:570–582

47. **Galet C, Ascoli M** 2006 A constitutively active mutant of the human lutropin receptor (hLHR-L457R) escapes lysosomal targeting and degradation. Mol Endocrinol 20:2931–2945

48. **Silveira LG, Noel SD, Silveira-Neto AP, Abreu AP, Brito VN, Santos MG, Bianco SD, Kuohung W, Xu S, Gryngarten M, Escobar ME, Arnhold IJ, Mendonca BB, Kaiser UB, Latronico AC** 2010 Mutations of the KISS1 gene in disorders of puberty. J Clin Endocrinol Metab 95:2276–2280

49. **Luan X, Yu H, Wei X, Zhou Y, Wang W, Li P, Gan X, Wei D, Xiao J** 2007 GPR54 polymorphisms in Chinese girls with central precocious puberty. Neuroendocrinology 86:77–83

50. **Luan X, Zhou Y, Wang W, Yu H, Li P, Gan X, Wei D, Xiao J** 2007 Association study of the polymorphisms in the KISS1 gene with central precocious puberty in Chinese girls. Eur J Endocrinol 157: 113–118